AUTOMATIC ARRHYTHMIA DETECTION BASED ON TIME AND TIME-FREQUENCY ANALYSIS OF HEART RATE VARIABILITY

M.G. Tsipouras and D.I. Fotiadis

19– 2002

Preprint, no 19 – 02 / 2002

Department of Computer Science
University of Ioannina
45110 Ioannina, Greece

AUTOMATIC ARRHYTHMIA DETECTION BASED ON TIME AND TIME-FREQUENCY ANALYSIS OF HEART RATE VARIABILITY

M.G. Tsipouras and D.I. Fotiadis

Unit of Medical Technology and Intelligent Information Systems,

Dept. of Computer Science, University of Ioannina, GR 45110, Ioannina, Greece

{markos, fotiadis}@cs.uoi.gr

ABSTRACT

We have developed an automatic arrhythmia detection system, which is based on heart rate features only. Initially, the RR interval duration signal is extracted from ECG recordings and segmented into small intervals. The analysis is based on both time and time-frequency features. Time domain measurements are extracted and several combinations between the obtained features are used for the training of a set of neural networks. Short time Fourier transform, and several time-frequency distributions are used in the time-frequency analysis. The features obtained are used for the training of a set of neural networks, one for each distribution. The proposed approach is tested using the MIT-BIH arrhythmia database and satisfactory results are obtained for both sensitivity and specificity (87.5% and 89.5%, respectively for time domain analysis and 90% and 93%, respectively for time-frequency domain analysis).

1. INTRODUCTION

Arrhythmia is a collective term for any cardiac rhythm, which deviates from the normal sinus rhythm. Arrhythmia may be due to a disturbance in impulse formation or conduction, or both, but it is not always an irregular heart activity [1]. Respiratory sinus arrhythmia is a natural periodic variation in RR intervals, corresponding to respiratory activity. Impulse formation may be sinus or ectopic, the rhythm regular or irregular and the heart rate fast, normal or slow [2,3]. Therefore, the detection of abnormal cardiac rhythms and automatic discrimination from the normal heart activity became an important task for clinical reasons. Most of the studies address the detection and identification of life threatening arrhythmias and specifically ventricular and atrial fibrillation and ventricular tachycardia. Various detection algorithms have been proposed, such as the sequential hypothesis testing [4], the multiway sequential hypothesis testing [7], the threshold-crossing intervals [5], the auto-correlation function [5], the VF-filter [5] and algorithms based on neural-networks [6,8,12]. Time-frequency analysis [9] and wavelet analysis [10,11] have also been used. Recent approaches utilize complexity measure [13] and multifractal analysis combined with a fuzzy Kohonen neural network [14].

Heart Rate Variability (HRV) refers to the beat-to-beat heart rate alterations. HRV believed to be a good marker of the individual's health condition and heart diseases [15]. Therefore, HRV analysis became a critical tool in cardiology for the diagnosis of heart diseases. Time domain analysis of the RR intervals includes the calculation of several common statistical indices [16,17] and the graphical representation of the RR interval duration signal [16,18]. Frequency analysis provides with the power spectrum density of the RR interval duration signal using Fourier transform and autoregressive techniques [16,19-23]. Time-frequency (t-f) analysis is based on the use of short time Fourier transform, time-frequency distributions

and wavelet analysis of the RR interval duration signal [24]. Other approaches for the HRV analysis include methods from nonlinear mathematics and chaos theory, such as fractal [24, 25] and approximate entropy [16, 25] analysis.

More specifically in the time – frequency analysis Wigner Ville (WV) distribution [26,27] and improved forms of WV, such as pseudo Wigner Ville (PWV) [28-31] and smoothed pseudo Wigner Ville (SPWV) [36-38], discrete Fourier transform and selective discrete Fourier transform [32-35], cone shaped kernel distribution [9], Choi-Williams distribution [39] and other exponential distributions [40] have been used.

In this paper we explore time and t-f analysis of the RR interval duration signal in order to detect arrhythmic segments of ECGs [41]. Initially, the RR interval duration signal is extracted from the ECG. The extracted signal is segmented into small intervals. The obtained signal is analyzed using both time and time-frequency features. For the time domain analysis selected time features are extracted. A set of neural networks is trained for all possible combinations among these features. Each combination of features is used for the training of one of the neural networks. Three decision rules are used to combine the outputs of all neural networks to obtain the final decision.

STFT and a number of TFDs such as WV, PWV, SPWV, Rihaczec, Page, Margenau-Hill, Bon Jordan and Zhao-Atlas-Marks distributions, are also applied and the obtained t-f characteristics are used for the training of a second set of neural networks. Each neural network corresponds to one of the above methods (STFT and TFDs) used. Finally, we apply three decision rules on the outputs of the set of the neural networks. In both cases the final

normal or arrhythmic outcome for a segment of the signal is not based on the result of a single identifier but on the combined outputs of a set of neural networks.

2. MATERIALS AND METHODS

Our analysis is carried out in four stages. First a preprocessing procedure is used to extract the tachograms from the ECGs. The tachograms are segmented into small segments. Each segment contains 32 RR intervals. In the second stage time domain or time-frequency methods are applied to extract the corresponding features. In the third stage the extracted features are used for the training of a set of neural networks. In the forth stage detection of arrhythmias is carried out using decision rules which are fed with the outputs of the neural networks.

A. Preprocessing

Preprocessing is carried out in two steps. In the first step we extract the tachograms from the ECG recordings. The dataset used in our study is the MIT-BIH arrhythmia database [45,46]. The database consists of 48 ECG recordings. The length of each recording is 30 minutes, which results to a total of 24 hours of recordings with 112,568 RR intervals. All RR intervals are used expect those close to the start or end of each recording which are excluded during segmentation. Each beat in the database is annotated with a character annotation (N, L, R, A, a, J, S, V, F, [, !,], e, j, n and E, P, f, p, Q, |, +, s, t and ~) . The beat annotations are explained in the database documentation [45]. The RDNN software, which accompanies the MIT-BIH database, is used for QRS detection. Then the RR interval duration signal (tachogram) can be obtained.

In the second step the tachograms are cut into small segments of 32 RR intervals each, and each segment is characterized as normal or arrhythmic using the MIT-BIH beat annotation. This results to 3,456 segments. For each RR interval the characterization of the second beat is used for its characterization. RR intervals with beat annotation N, P, f, p, Q, |, +, s, t and ~ were characterized as "Normal" and RR intervals with beat annotation L, R, A, a, J, S, V, F, [, !,], e, j, n and E were characterized as "Arrhythmic". A 32 RR interval segment is characterized "Normal" if it contains more than 95% "Normal" RR intervals, otherwise is characterized "Arrhythmic". The preprocessing scheme is shown in Fig.1.

B. Time domain analysis

We apply time domain analysis on the segmented dataset. Time domain analysis results in indices and markers obtained from the tachogram, such as mean and standard deviation of RR intervals, mean and standard deviation of differences between adjacent RR intervals, difference between the longer and the shorter RR interval etc. The standard deviation of all normal - to - normal RR intervals (SDRR) is the simplest feature that can be extracted from the tachogram.

$$SDRR = \sqrt{\sum_{i=1}^{N} (RR_i - \mu)^2} \quad (1)$$

$$\mu = \sum_{i=1}^{N} \frac{RR_i}{N} \quad (2)$$

where N is the total number of the RR intervals, RR_i is the duration o f the i^{th} RR interval and μ is the mean value. The root mean square of successive differences of all normal - to -

normal RR intervals (r_MSSD) and the standard deviation of successive differences of all normal - to - normal RR intervals (SDSD) are also widely used indices.

$$\text{r\_MSSD} = \sqrt{\sum_{i=1}^{N-1} \frac{(RR_i - RR_{i+1})^2}{N-1}}, \tag{3}$$

$$\text{SDSD} = \sqrt{\sum_{i=1}^{N-1} ((RR_{i+1} - RR_i) - d\mu)^2}, \tag{4}$$

$$d\mu = \sum_{i=1}^{N-1} \frac{RR_i - RR_{i+1}}{N-1}, \tag{5}$$

where $d\mu$ is the mean value of successive differences of the RR intervals. The percentage of intervals presenting time duration difference between adjacent normal-to-normal RR intervals greater than 50msec (pNN50) is another HRV characteristic. In many studies this percentage is used with different time threshold, such as 5msec (pNN5) or 10 msec (pNN10), i.e.

$$\text{pNNx} = \frac{\text{number of time duration differences of succesive RR intervals} > \text{x msec}}{N-1}. \tag{6}$$

The normal-to-normal RR intervals are all intervals between adjacent QRS complexes resulting from sinus node depolarization [15].

We use all possible combinations among the above mentioned time analysis features (each combination contains 1, 2, 3, 4, 5 or 6 features) to create the pattern set for the classification stage. This leads to a total of 63 feature combinations, which are shown in Table 1, with 3,426 patterns each. In the third stage (classification stage) we train a feed-forward back-

propagation neural network, for each feature combination. We use 1,426 patterns randomly chosen from the total of 3,426 patterns as training set. Several neural network architectures have been tried and we have chosen the one that performs better: N inputs (number of features used in the specific combination), one hidden layer with 20 neurons and one output, being a real number between 0 and 1. The final "Normal" or "Arrhythmic" classification is made with 0.5 threshold on the networks' output. The training of the neural network ends when the square error is less than 0.01 or the training epochs are more than 2000. The procedure followed for the time domain features is shown in Fig. 2. Finally, we result in a set with 63 neural networks (one for each combination). The outputs of the neural networks are fed into a set of decision rules as it is described below (forth stage).

C. Time-frequency analysis

STFT and various time-frequency distributions (TFDs) is used for the time-frequency analysis of the segmented dataset. For STFT the signal $x(u)$ is pre-windowed around a time instant t, and the Fourier Transform if calculated for each time instant t.

$$STFT(t,f) = \int_{-\infty}^{+\infty} x(\tau)h(\tau - t)e^{-if\tau}d\tau \qquad (7)$$

where h(t) is a short time window, localized around t = 0 and f = 0, and x(t) the signal. STFT suffers of trade-off between its window length and its frequency resolution. The TFDs used in our study belong to the Cohen's class of distributions [42,43] and are given by the following formula

$$\rho(t,f) = \iiint e^{i2\pi\upsilon(u-t)} g(\upsilon,\tau) s^*\left(u-\frac{1}{2}\tau\right) s\left(u+\frac{1}{2}\tau\right) e^{-i2\pi f\tau} d\upsilon\, du\, d\tau \qquad (8)$$

where $s(t)$ is the time signal, $s^*(t)$ is its complex conjugate and $g(\upsilon,\tau)$ is an arbitrary function called kernel. The kernel is different for each TFD. Table 2 shows selected TFDs which are used in our study and the corresponding kernels [42-44,48,49].

For each 32 RR interval segment STFT and all TFDs are applied (totally 19 methods). The Power Spectrum Density (PSD) is computed and normalized in the [-1,1] interval for amplitude. This represents the fractional energy of the signal in time t and frequency f (Fig. 3a). We obtain horizontal slices from the PSD for amplitude = 0.0, 0.2, 0.4, 0.6, 0.8 and 1.0 which contain the corresponding PSD trace (Fig. 3b). The areas between adjacent slide traces are calculated (Fig. 3c and 3d). These areas are the time-frequency features. Six features for each TFD are computed. They are used for the training of the neural networks.

For STFT and each TFD we train a feed-forward back-propagation neural network, using 1,426 patterns randomly chosen from the total of 3,426 patterns as training set. The architecture is similar to the one used in time-domain analysis: six inputs, one hidden layer with 20 neurons and one output being a real number in the interval [0,1]. The analysis based on time-frequency features is presented in Fig. 4. Finally, we result in a set with 19 neural networks (one for each method). The outputs of the neural networks are fed into a set of decision rules (forth stage), which is common for both procedures.

D. Arrhythmia Detection

For both time domain and t-f analysis we use the remaining 2,000 segments of the segmented dataset as test set. The outputs from all neural networks trained for each approach (63 for time domain analysis and 19 for t-f analysis) are fed into the following decision rules to obtain the final decision for each segment (normal or arrhythmic).

- Average: For each segment we calculate the average of the outputs of all neural networks and a threshold 0.5 is used for the final decision, i.e.

$$T = \begin{cases} \text{Normal (0)} & \text{if } \dfrac{\sum_{i=1}^{N} y_i}{N} \le 0{,}5 \\ \text{Arrhythmic (1)} & \text{if } \dfrac{\sum_{i=1}^{N} y_i}{N} > 0{,}5 \end{cases}, \tag{9}$$

where T is the final decision, N is the number of the neural networks and y_i is the output of the i^{th} neural network

- Vote: For each segment all neural networks vote if it is arrhythmic, with threshold 0.5, i.e.

$$A_i = \begin{cases} 0 & \text{if } y_i \le 0{,}5 \\ 1 & \text{if } y_i > 0{,}5 \end{cases}$$

where y_i is the output of the i^{th} neural network and A_i the vote of the i^{th} neural network. If more than half votes are accumulated then the decision is "Arrhythmic", otherwise "Normal", i.e.

$$T = \begin{cases} \text{Normal (0)} & \text{if } \sum_{i=1}^{N} A_i \le \dfrac{N}{2} \\ \text{Arrhythmic (1)} & \text{if } \sum_{i=1}^{N} A_i > \dfrac{N}{2} \end{cases}. \tag{10}$$

- Decision Vote: Each neural network "decides" if it will vote using

$$\Psi_i = \begin{cases} 0 & \text{if } |y_i - 0.5| \le 0.1 \\ y_i & \text{if } |y_i - 0.5| > 0.1 \end{cases}, \tag{11}$$

where y_i is the output of the i^{th} neural network and Ψ_i the vote of the i^{th} neural network. If all neural networks vote 0 for a segment then the vote is calculated as:

$$\Psi_i = y_i, \tag{12}$$

The average of all votes is used with threshold 0.5 for the final decision, i.e.

$$T = \begin{cases} \text{Normal}\,(0) & \text{if } \dfrac{\sum_{i=1}^{N} \Psi_i}{N} \le 0.5 \\ \text{Arrhythmic}\,(1) & \text{if } \dfrac{\sum_{i=1}^{N} \Psi_i}{N} > 0.5 \end{cases}. \tag{13}$$

The architecture of the neural networks used is shown in Fig. 5. The transfer function used among the layers is the hyperbolic tangent sigmoid function. The training function is the Levenberg-Marquardt back propagation method [47]. We use the mean squared error performance function, which measures the network's performance using the mean of squared errors.

3. RESULTS

The corresponding sensitivity and specificity for each neural network is computed. The results for sensitivity and specificity, for the 63 neural networks trained with time feature combinations and the 19 neural networks trained with time-frequency features, are reported in Tables 3a and 3b, respectively. The results for a single neural network are not satisfactory (average sensitivity and specificity: 74% and 72% for neural networks trained with time features and 74% and 78% for neural networks trained with time-frequency features).

Therefore a single neural network cannot be used for arrhythmia detection. We have observed the following:

1. Each neural network results in high sensitivity and specificity for signal segments for which the output is less than 0.3 or higher than 0.7. This is because the output of the neural network can be viewed as a possibility function that decides if a segment is normal (result 0) or arrhythmic (result 1).
2. Each neural network results in low sensitivity and specificity for signal segments for which the output was near 0.5 (i.e. in the interval $[0.5 - k, 0.5 + k]$ with $k \leq 0.2$). This is an uncertainty interval with high error rate.
3. A number of neural networks detected correctly almost all signal segments with output outside the uncertainty interval [0.45, 0.55] (i.e. $k=0.05$). When the uncertainty interval is larger (i.e. $k = 0.1, 0.15$ or 0.2) the number of neural networks which detect the same number of segments correctly is reduced. In this case for some segments there are no neural networks with output outside the uncertainty interval. We have used various uncertainty intervals and the best choice is [0.4, 0.6] (i.e. $k = 0.1$).

The above observations lead us to use multiple identifier combined with decision rules. The results for sensitivity and specificity when we use the decision rules on the neural networks' outputs are presented in Table 4. For each decision rule the Receiver Operating Characteristic (ROC) curve is computed. The ROC curves are shown in Fig. 6. Using the ROC curves the Area Under Curve (AUC) marker is calculated and the results are presented in Table 5.

4. DISCUSSION - CONCLUSIONS

We have developed an automatic procedure for the detection of arrhythmias using ECG recordings. The method comprises of four stages. In the first the ECG signal is transformed to the RR interval duration signal which is segmented into small segments of 32 RR intervals each. In the second features of those segments are extracted. In the third a set of neural networks is trained. In the forth the outputs of the neural networks are fed into decision rules. The outcome of the method is the classification of segments in normal or arrhythmic.

The method is based on time analysis and time frequency analysis features which are obtained in the second stage. If time features were chosen then their combination leads to 63 neural networks. If time frequency analysis was followed then we result into 19 neural networks. We have proven that a single neural network does not provide with satisfactory results in terms of sensitivity and specificity and this imposed the use of decision rules. One of the advantages of the method is that using only heart rate features can lead to the identification of arrhythmic intervals in ECG recordings. This is independent of the type of arrhythmia. In the past several researchers have addressed similar problems, as it is shown in Table 6, but they have identified only some types of arrhythmia and in smaller datasets. The obtained sensitivity and specificity refers to the whole MIT-BIH database which in our analysis has been segmented into 3,426 segments of 32 RR intervals.

For the time domain approach the average and vote decision rules result in low performance for both sensitivity and specificity (81% and 78%, respectively). This is expected since in both cases the neural networks' outputs inside the uncertainty interval have high error rate. The sensitivity and specificity for decision vote are 87.5% and 89.5 %, respectively. Average and vote decision rules for the time frequency features resulted in 87% sensitivity and 89% specificity. The decision vote results are better (90% sensitivity and 93% sensitivity).

In our study besides the QRS detection and the extraction of the RR interval duration signal, there is no other processing of the ECG recording (such as P wave or T wave detection which will make the process more complicated and time consuming). Therefore, noisy data can be analyzed because QRS detection algorithms perform well. The exclusive use of the RR interval duration signal leads to a high reduction of input and processing data, compared to other ECG analysis methods.

Moreover, the final decision is not based on a single identifier but on the combined results of a set of identifiers. Therefore, the system is expected to have high generalization capability. Due to the short processing time and the generalization capability of the method we believe that the proposed approach can be used in real time arrhythmia detection systems. In addition, RR interval duration features can be used for the classification of detected arrhythmic segments into several arrhythmia types.

Acknowledgements

The authors are grateful to Prof. D. Sideris and Prof. A. Likas for useful comments and suggestions.

5. REFERENCES

[1] E. Sandoe, B. Sigurd, Arrhythmia - A guide to clinical electrocardiology, Publishing Partners Verlags GmbH, Bingen, 1991.

[2] L. and E. Goldberger, Clinical Electrocardiography, The Mosby Company, Saint Louis, 1977.

[3] D.A. Sideris, Primary Cardiology, Scientific Editions Grigorios K. Parisianos, Athens, 1991 (in Greek).

[4] N.V. Thakor, Y.S. Zhu, K.Y. Pan, Ventricular tachycardia and fibrillation detection be a sequential hypothesis testing algorithm, IEEE Trans. Biom. Eng. 37 (9) (1990) 837-843.

[5] R.H. Clayton, A. Murray, R.W.F. Campbell, Comparison of four techniques for recognition of ventricular fibrillation of the surface ECG, Med. Biol. Eng. Comp. 31 (1993) 111-117.

[6] R.H. Clayton, A. Murray, R.W.F. Campbell, Recognition of ventricular fibrillation using neural networks, Med. Biol. Eng. Comp. 32 (1994) 217-220.

[7] N.V. Thakor, A. Natarajan, G. Tomaselli, Multiway sequential hypothesis testing for tachyarrhythmia discrimination, IEEE Trans. Biom. Eng. 41 (5) (1994) 480-487.

[8] T.F. Yang, B. Device, P.W. Macfarlane, Artificial neural networks for the diagnosis of atrial fibrillation, Med. Biol. Eng. Comp. 32 (1994) 615-619.

[9] V.X. Afonso, W.J. Tompkins, Detecting ventricular fibrillation, IEEE Eng. Med. Biol. (1995) 152-159.

[10] L. Khadra, A.S. Al-Fahoum, H. Al-Nashash, Detection of life-threatening cardiac arrhythmias using wavelet transformation, Med. Biol. Eng. Comp. 35 (1997) 626-632.

[11] A.S. Al-Fahoum, I. Howitt, Combined wavelet transformation and radial basis neural networks for classifying life-threatening cardiac arrhythmias, Med. Biol. Eng. Comp. 37 (1999) 566-573.

[12] K. Minami, H. Nakajima, T. Toyoshima, Real-time discrimination of ventricular tachyarrhythmia with Fourier-transform neural network, IEEE Trans. Biom. Eng. 46 (2) (1999) 179-185.

[13] X.S. Zhang, Y.S. Zhu, N.V. Thakor, Z.Z. Wang, Detecting ventricular tachycardia and fibrillation by complexity measure, IEEE Trans. Biom. Eng. 46 (5) (1999) 548-555.

[14] Y. Wang, Y.S. Zhu, N.V. Thakor, Y.H. Xu, A short-time multifractal approach for arrhythmia detection based on fuzzy neural network, IEEE Trans. Biom. Eng. 48 (9) (2001) 989-995.

[15] Task force of The European Society of Cardiology and The North American Society of Pacing and Electrophysiology, Heart Rate Variability: Standards of measurement, physiological interpretation and clinical use, Eur. Heart J. 17 (1996) 354-381.

[16] M. Malik, A.J. Camm, Heart Rate Variability, Futura Publishing Company, New York, 1995.

[17] R. Kleiger, P. Stein, M. Bosner, J. Rottman, Time Domain measurement of Heart Rate Variability, Cardiol. Clin. 10 (1992).

[18] F. Azuaje, W. Dubitzky, P. Lopes, N. Black, K. Adamson, X. Wu, J.A. White, Predicting coronary disease risk based on short-term RR interval measurements: a neural network approach, Artif. Int. Med, 15 (3) (1999) 275-297.

[19] C. Albrecht, Estimation of heart rate power spectrum bands from real world data: dealing with ectopic beats with noisy data, Comp. in Cardiol. (1988).

[20] A. Malliani, M. Pagani, F. Lombardi, S. Cerrutti Cardiovascular neural regulation explored in the frequency domain, Circ. 84 (2) (1991) 482-492.

[21] J.T. Bigger, Jr.JL. Fleiss, R.C. Steinman, L.M. Rolnitzky, R.E. Kleiger, J.N. Rottman Frequency domain measures of heart period variability and mortality after myocardial infarction, Circ. 85 (1) (1992) 164-171.

[22] A.M. Bianchi, L.T. Mainardi, E. Petrucci, M.G. Signorini, M. Mainardi, and S. Cerutti, Time-variant power spectrum analysis for the detection of transient episodes in HRV signal, IEEE Trans Biomed Eng, 40 (1993) 136-144.

[23] L. Basano, F. Canepa, P. Ottonello, Real time spectral analysis of HRV signals: an interactive and user- friendly PC system, Comp. Meth. and Progr. in Biomed. 55 (1) (1998) 69-76.

[24] M. Akay, Time Frequency and wavelets in biomedical signal processing, IEEE Press, 1998.

[25] T. Mekikallio, Analysis of Heart Rate Dynamics by Methods Derived from Nonlinear Mathematics, Oulu University Library, Oulu, 1999.

[26] V. Novak, P. Novak, J. de Champlain, A.R. Le Blanc, R. Martin, R. Nadeau, Influence of respiration on heart rate and blood pressure fluctuations, J. Appl. Physiol. 74 (2) (1993) 617-626.

[27] P. Novak, V. Novak, Time/frequency mapping of the heart rate, blood pressure and respiratory signals, Med. Biol. Eng. Comput. 31 (2) (1993) 103-110.

[28] V. Novak, P. Novak, M. deMarchie, R. Schondorf, The effect of severe brain stem injury on heart rate and blood pressure oscillation, Clin. Auton. Res. 5 (1) (1995) 24-30.

[29] V. Novak, P. Novak, T.L. Opfer-Gehrking, P.A. Low, Postural tachycardia syndrome: time frequency mapping, J. Auton. Nerv. Syst. 61 (3) (1996) 313-320.

[30] A. Bharucha, V. Novak, M. Camilleri, A.Z. Zinsmeister, R.B. Hanson, P.A. Low, a^2-Adrenergic modulation of colonic tone during hyperventilation, Am. J. Physiol. (1997) 273.

[31] V. Novak, A.L. Reeves, P. Novak, P.A. Low, F.W. Sharbrough, Time-frequency mapping of R-R interval during complex partial seizures of temporal lobe origin, J. Auton. Nerv. Syst. 77 (2-3) (1999) 195-202.

[32] S. Akselrod, D. Gordon, F.A. Ubel, D.C. Shannon, A.C. Barger, R.J. Cohen, Power spectrum analysis of heart rate fluctuation: a quantitative probe of beat to beat cardiovascular control, Science 213 (1981) 220–222.

[33] L. Keselbrener, A. Baharav, S. Akselrod, Estimation of fast vagal response by time-dependent analysis of heart rate variability in normal subjects, Clin. Auton. Res. 6 (6) (1996) 321-327.

[34] L. Keselbrener, S. Akselrod, Selective discrete Fourier transform algorithm for time-frequency analysis: method and application on simulated and cardiovascular signals, IEEE Trans. Biomed. Eng. 43 (8) (1996) 789-802.

[35] L. Keselbrener, S. Akselrod, Time-frequency analysis of transient signals - application to cardiovascular control, Physica A. 249 (1-4) (1998) 482-490.

[36] H.H. Huang, H.L. Chan, P.L. Lin, C.P. Wu, C.H. Huang, Time-frequency spectral analysis of heart rate variability during induction of general anaesthesia, Br. J. Anaesth. 79 (6) (1997) 754-758.

[37] H.L. Chan, J.L. Lin, C.C. Du, C.P. Wu, Time-frequency distribution of heart rate variability below 0.05 Hz by Wigner-Ville spectral analysis in congestive heart failure patients, Med. Eng. Phys. 19 (6) (1997) 581-587.

[38] H.L. Chan, J.L. Lin, H.H. Huang, C.P. Wu, Elimination of interference component in Wigner-Ville distribution for the signal with 1/f spectral characteristic, IEEE Trans. Biomed. Eng. 44 (9) (1997) 903-907.

[39] F. Claria, M. Vallverdu, R. Baranowski, L. Chojnowska, P. Caminal, Time-frequency analysis of the RT and RR variability to stratify hypertrophic cardiomyopathy patients, Comp. Biomed. Res. 33 (4) (2000) 416-430.

[40] H.G. Steenis, J.H.M. Tulen, The exponential distribution applied to nonequidistandly sampled cardiovascular time series, Comp. Biomed. Res. 29 (1996) 174-193.

[41] S. Stamatelopoulos, D. Sideris, L. Anthopoulos, S. Moulopoulos, Observations for a new study method for characteristics of cardiac disease, Proc. of the Athens Medical Society, C' (1970) 284-296 (in Greek).

[42] L. Cohen, Time-frequency distributions – A review, Proc. of IEEE, 77 (7) (1989) 941-981.

[43] B. Boashash, Time-frequency signal analysis, Wiley, 1992.

[44] A. Papandreou, G.F. Bourdreaux-Bartels, Generalization of the Choi-Williams Distribution and the Butterworth Distribution for Time-Frequency Analysis, IEEE Trans. Sig. Proc. 41 (1) (1993) 463-472.

[45] MIT-BIH Arrhythmia Database CD-ROM, Third Edition, Harvard-MIT Division of Health Sciences and Technology, 1997.

[46] G.B. Moody, R.G. Mark, The impact of the MIT-BIH arrhythmia database, Comp. Biomed. Res. 29 (1996) 174-193.

[47] Neural Network Toolbox, ver 3.0, Mathworks Inc. 1992-1997

[48] F. Auger, P. Flandrin, P. Goncalves, O. Lemoine, Time-Frequency Toolbox Tutorial, CNRS (France) - RICE University (USA), 1995-1996.

[49] F. Auger, P. Flandrin, P. Goncalves, O. Lemoine, Time-Frequency Toolbox Reference Guide, CNRS (France) - RICE University (USA), 1995-1996.

FIGURE 1

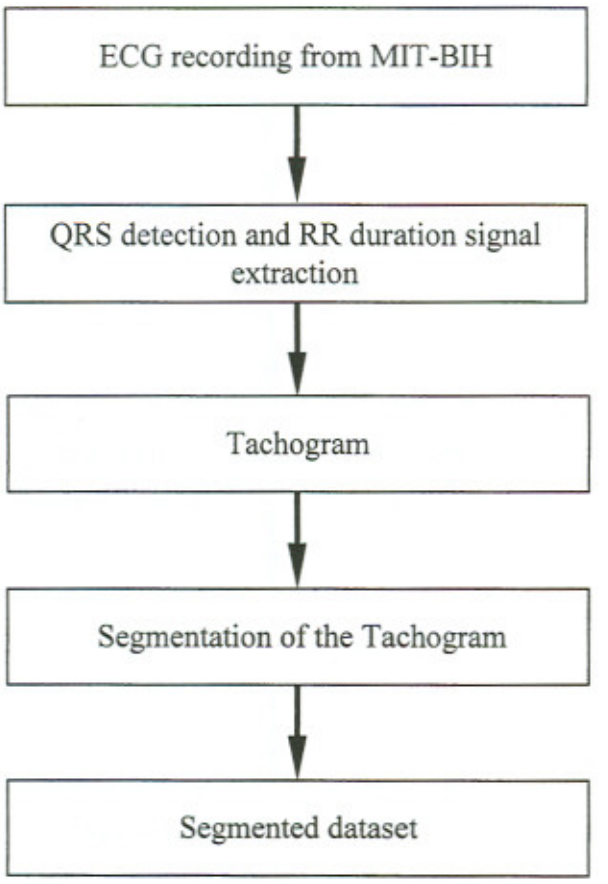
ECG recording from MIT-BIH
QRS detection and RR duration signal extraction
Tachogram
Segmentation of the Tachogram
Segmented dataset

FIGURE 2

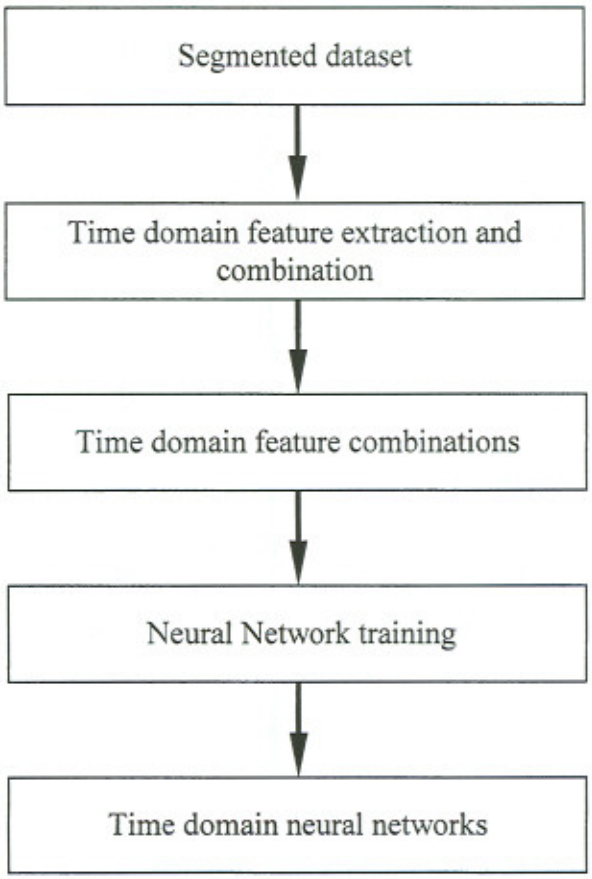
Segmented dataset
Time domain feature extraction and combination
Time domain feature combinations
Neural Network training
Time domain neural networks

FIGURE 3 (a,b,c,d)

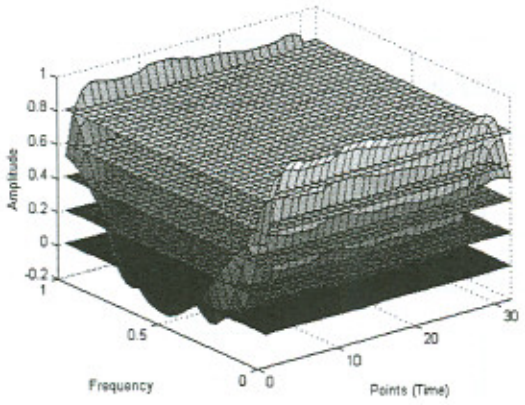

(a)

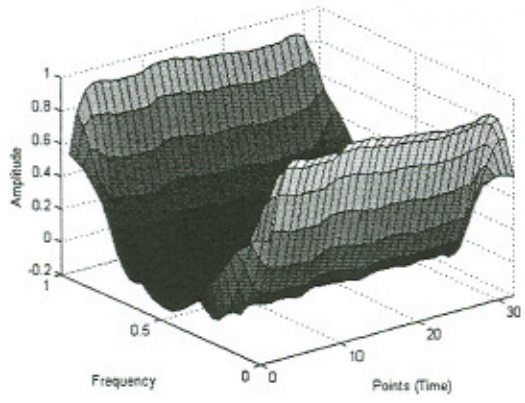

(b)

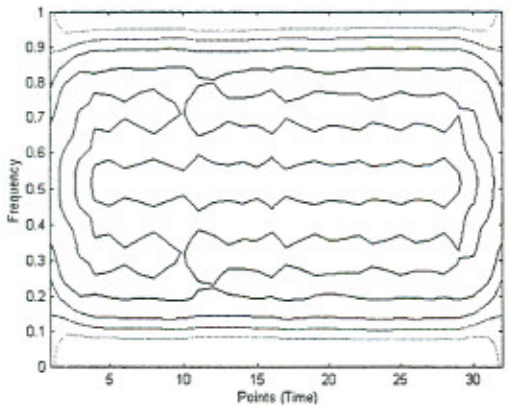

(c)

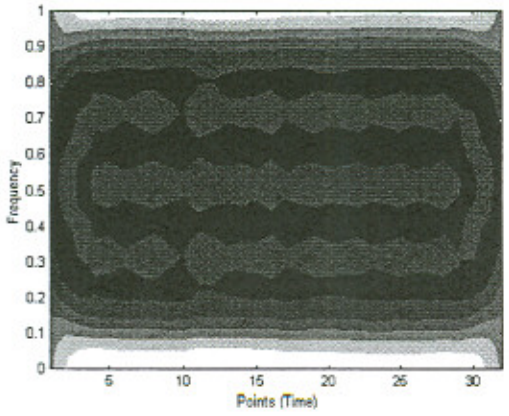

(d)

FIGURE 4

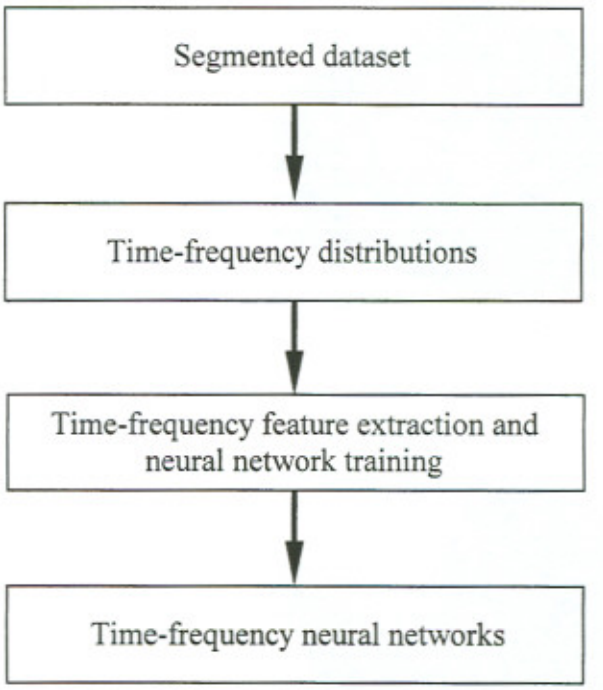
Segmented dataset
Time-frequency distributions
Time-frequency feature extraction and neural network training
Time-frequency neural networks

FIGURE 5

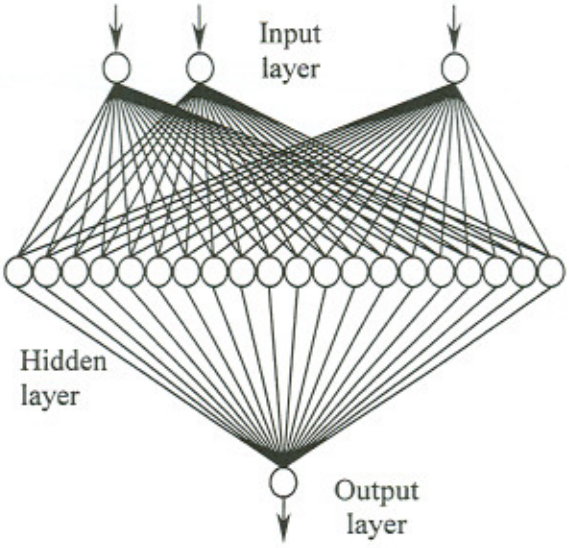

FIGURE 6 (a,b)

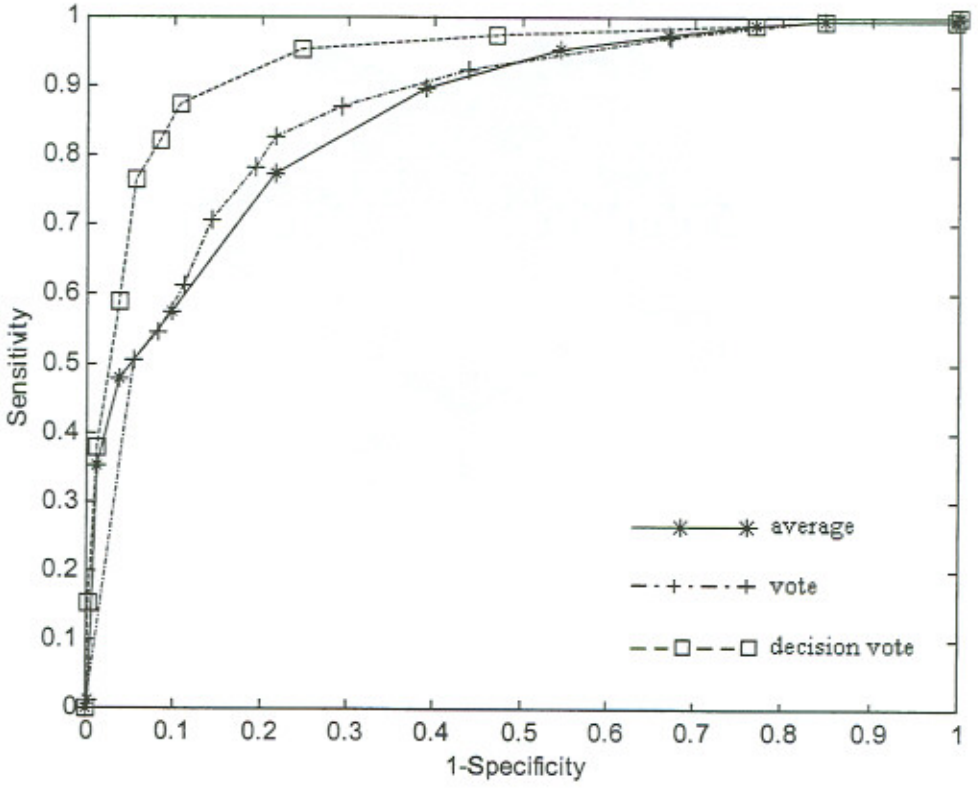

(a)

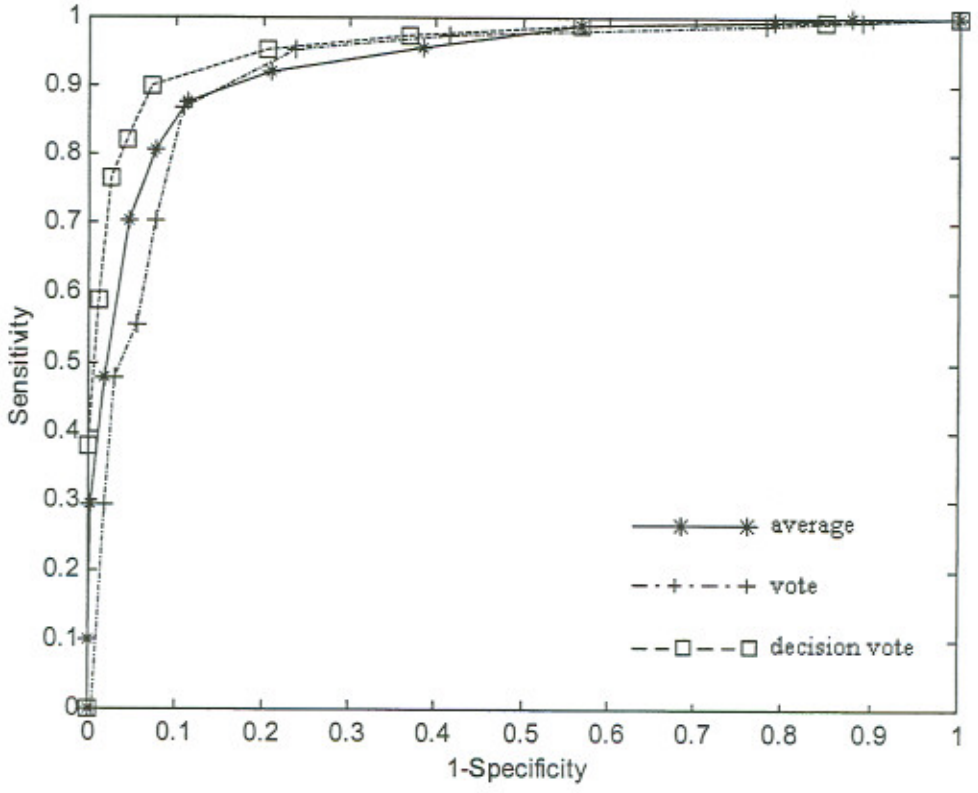

(b)

FIGURE LEGENDS

Figure 1. Preprocessing of the ECG signal

Figure 2. Time domain analysis.

Figure 3. a. Time-frequency distribution, b. Horizontal slices, c. Traces, d. Features for time-frequency methods

Figure 4. Time-frequency analysis.

Figure 5. Architecture of the neural network.

Figure 6. a. ROC curve for decision rules for neural networks trained with time features

b. ROC curve for decision rules for neural networks trained with time-frequency features

Table 1. Combinations of time domain features.

	Feature Combination	Features
1	1	SDNN
2	2	r_MSSD
3	12	SDNN, r_MSSD
4	3	SDSD
5	13	SDNN, SDSD
6	23	SDNN, r_MSSD
7	123	SDNN, r_MSSD, SDSD
8	4	pNN5
...	...	...
60	3456	SDSD, pNN5, pNN10, pNN50
61	13456	SDNN, SDSD, pNN5, pNN10, pNN50
62	23456	r_MSSD, SDSD, pNN5, pNN10, pNN50
63	123456	SDNN, r_MSSD, SDSD, pNN5, pNN10, pNN50

Table 2. Time-frequency distributions.

	Distribution	Kernel ($g(\upsilon,\tau)$)	
1	Born-Jordan	$\frac{\sin(\pi\upsilon\tau)}{\pi\upsilon\tau}$	
2	Butterworth	$\frac{1}{1+\left(\frac{\upsilon}{\upsilon_1}\right)^{2N}\left(\frac{\tau}{\tau_1}\right)^{2M}}$	$N,M,\upsilon_1,\tau_1 > 0$
3	Choi-Williams	$e^{\frac{-(\pi\upsilon\tau)^2}{2\sigma^2}}$	σ : scaling factor
4	Generalized rectangular	$\frac{\sin\left(\frac{2\pi\sigma\upsilon}{\lvert\tau\rvert^{\alpha}}\right)}{\pi\upsilon}$	σ : scaling factor a : dissymmetry ratio
5	Margenau-Hill	$\cos(\pi\upsilon\tau)$	
6	Pseudo Margenau-Hill	$h(\tau)\cos(\pi\upsilon\tau)$	$h(\tau)$: window function
7	Margenau-Hill-Spectrogram	$h(\tau)\cos(\pi\upsilon\tau)\ A_x^*(\upsilon,\tau)$	$A_x(\upsilon,\tau)$: Ambiguity function
8	Page	$e^{j\pi\upsilon\lvert\tau\rvert}$	
9	Pseudo Page	$h(\tau)\,e^{j\pi\upsilon\lvert\tau\rvert}$	$h(\tau)$: window function
10	Wigner-Ville	1	
11	Pseudo Wigner-Ville	$h(\tau)$	$h(\tau)$: window function
12	Smoothed Pseudo Wigner-Ville	$G(\upsilon)\,h(\tau)$	$h(\tau)$: window function
13	Rihaczek	$e^{j\pi\upsilon\tau}$	
14	Reduced interference (Bessel window)	$\int_{-\infty}^{+\infty} h(t)e^{-j2\pi\upsilon\tau t}dt$	h(t) : Bessel window
15	Reduced interference (Hanning window)	$\int_{-\infty}^{+\infty} h(t)e^{-j2\pi\upsilon\tau t}dt$	h(t) : Hanning window
16	Reduced interference (Binomial window)	$\int_{-\infty}^{+\infty} h(t)e^{-j2\pi\upsilon\tau t}dt$	h(t) : Binomial window
17	Reduced interference (Triangular window)	$\int_{-\infty}^{+\infty} h(t)e^{-j2\pi\upsilon\tau t}dt$	h(t) : Triangular window
18	Zhao-Atlas-Marks	$h(\tau)\frac{\sin(\pi\upsilon\tau)}{\pi\upsilon\tau}$	$h(\tau)$: window function

Table 3a. Results for sensitivity and specificity for neural networks trained with time features.

Combination	Sensitivity	Specificity	Combination	Sensitivity	Specificity
1	74%	62%	6	85%	47%
2	60%	86%	16	74%	66%
12	77%	76%	26	74%	76%
3	60%	86%	126	77%	80%
13	76%	74%	36	73%	77%
23	69%	77%	136	79%	75%
123	77%	75%	236	72%	76%
4	74%	44%	1236	80%	77%
14	72%	65%	46	81%	49%
24	69%	76%	146	74%	65%
124	74%	75%	246	75%	75%
34	62%	84%	1246	77%	77%
134	77%	75%	346	76%	76%
234	68%	79%	1346	79%	77%
1234	76%	71%	2346	73%	75%
5	83%	40%	12346	75%	78%
15	69%	69%	56	79%	49%
25	71%	73%	156	73%	67%
125	73%	76%	256	72%	78%
35	68%	79%	1256	75%	79%
135	75%	77%	356	76%	73%
235	69%	81%	1356	77%	77%
1235	79%	76%	2356	73%	76%
45	81%	40%	12356	78%	78%
145	69%	67%	456	76%	53%
245	70%	72%	1456	73%	70%
1245	75%	74%	2456	74%	75%
345	66%	77%	12456	80%	72%
1345	76%	75%	3456	77%	72%
2345	71%	78%	13456	73%	77%
12345	78%	71%	23456	75%	74%
			123456	78%	72%

Table 3b. Results for sensitivity and specificity for neural networks trained with t-f features.

Distribution	Sensitivity	Specificity
Born-Jordan	72%	74%
Butterworth	71%	78%
Choi-Williams	76%	73%
Generalized Rectangular	74%	80%
Margenau-Hill	73%	76%
Pseudo Margenau-Hill	74%	76%
Margenau-Hill	80%	82%
Page	74%	84%
Pseudo Page	80%	84%
Wigner-Ville	69%	76%
Pseudo Wigner-Ville	70%	84%
Smoothed pseudo Wigner-Ville	75%	82%
Rihaczek	75%	80%
Reduced Interference (Bessel Window)	76%	79%
Reduced Interference (Hanning Window)	75%	72%
Reduced Interference (Binomial Window)	71%	76%
Reduced Interference (Triangular Window)	73%	76%
Zhao-Atlas-Marks	80%	78%
STFT	70%	73%

Table 4. Results for sensitivity and specificity for decision rules.

Time domain analysis

Decision Rule	Sensitivity	Specificity
Average	80.68%	78.18%
Vote	82.60%	78.43%
Decision Vote	87.53%	89.48%

Time-frequency analysis

Decision Rule	Sensitivity	Specificity
Average	87.64%	88.65%
Vote	86.84%	89.25%
Decision Vote	89.95%	92.91%

Table 5. AUC marker results for decision rules.

	AUC marker	
Decision Rule	Time	t-f
Average	85,91%	85,91%
Vote	86,32%	86,32%
Weight Vote	93,46%	93,46%

Table 6. AUC marker results for decision rules.

Author	Dataset	Results	Sens.	Spec.
Thakor – Zhu Pan	170 records (8 sec)	100% identification after 7 sec.		
Clayton -Muray Campbell	70 extracts (4 sec)	Threshold Crossing Intervals	46%	72%
		Autocorrelation Function	67%	38%
		VF Filter Leakage	77%	55%
		Signal Spectrum Shape	53%	93%
Clayton - Muray Campbell	70 extracts (4 sec)	Neural Networks	84%	59%
Yang - Device MacFariane	3080 ECGs		92%	93%
Khadra AlFahoum AlNashash	45 ECGs 8 NR, 12 VF, 13 VT, 12 AF	Ventricular Fibrillation	91,7%	83,3%
		Atrial Fibrillation	91,7%	91,7%
		Ventricular Tachycardia	84,6%	92,3%
		Normal Rhythm	87,5%	87,5%
AlFahoum Howitt	158 ECGs 37 NR, 49 VF, 49 VT, 20 AF	Ventricular Fibrillation	100%	100%
		Atrial Fibrillation	95,2%	85,7%
		Ventricular Tachycardia	100%	100%
		Normal Rhythm	92,5%	97,5%
Minami Nakajima Toyashima	700 QRS 150 VT, 250 VF, 300 NR	Ventricular Fibrillation	92%	92%
		Ventricular Tachycardia	80%	96%
		Normal Rhythm	99%	98%
Zhang - Zhu Thakor - Wang	170 records (48 sec) 85 VT, 85 VF, 34 NR	100% identification after 7 sec.		
Wang - Zhu Thakor - Xu	180 records (6 sec) 60 VF, 60 AF, 60 VT	Ventricular Fibrillation	98,3%	96,7%
		Ventricular Tachycardia	95%	99,2%
		Atrial Fibrillation	98,3%	100%
This work	MIT-BIH Arrhythmia database 48 ECGs 30 min. length 112.568 beats	All types included in MIT-BIH	87,53%	89,48%
			89,95%	92,91%